

## Double Diffusion in Enclosure Bounded by Massive and Volatilizing Walls

Di Liu  
Doctoral  
Candidate

Guangfa Tang  
Professor

Fuyun Zhao  
Doctoral  
Candidate

College of Civil Engineering, Hunan University, Changsha, P. R. China

liudi66@163.com

**Abstract:** Hazard volatilization emitted from walls enters into airflow in the room, making the indoor air quality worse. An exterior wall of some thickness is affected on its surface by the outdoor air environment. In this paper, conjugated double diffusive natural convection in square enclosure bounded by massive and volatilizing walls is numerically studied. Various parameters, including dimensionless heat and mass conductivities of the bounding wall ( $Rt$  and  $Rc$ ,  $10^{-4}$ -10.0) and Buoyancy ratio ( $N$ , 0-10), are considered. Other governing parameters are maintained constant (Rayleigh number, Prandtl number, Lewis number and width ratio of massive wall to enclosure). The conjugate heat transfer of the thick wall and indoor airflow and the enhanced heat transfer and combined double diffusion are analyzed. The isotherms, concentration, streamlines or flow charts, and wall Nusselt numbers are produced for various cases, which should be interest for design of indoor environments and selection of building materials.

**Key Words:** Double diffusion; Conjugate heat transfer; Opposition

### 1. INTRODUCTION

It has become evident that building products are major contributors to the pollution of the indoor air environment with volatile organic compounds (VOCs) [1]. The indoor airflow and temperature distributions also have influence on the emission rates of VOCs. Then the study of indoor air quality should be concentrated on the pollutants, thermal sources and their concentration levels [2]. At the same time, Concentration and temperature gradients caused by the contaminant source and thermal source induce

double diffusive natural convection. Double diffusive natural convection in rooms has been a problem studied to some extent [3-5]. On the other hand, the walls of building separate the internal room and the external space. The conjugate heat transfer is encountered in the real life and studied by many authors. Liaqat and Baytas analyzed the laminar natural convection flow in a square enclosure having thick conducting walls [6], similar work done by Kim and Viskanta though the internal heat source not being considered [7]. Desrayaud and Lauriat studied natural convection in partially open enclosures with a conducting side-wall, and found that a boundary layer was formed adjacent to the cold wall and the mean temperature of the bounding wall approaches that of the hot fluid [8]. Yedder and Bilgen also calculated conjugate heat transfer in enclosure though turbulence was included [9].

In this paper, authors would aim at double diffusion and conjugate heat transfer in a square enclosure bounded by vertical massive and volatilizing walls. Influence of outdoor radiation and airflow is taken into surface heat flux of the massive wall account. Various parameters, including Rayleigh number (derived from air and hazard gas), Lewis numbers, dimensionless conductivity of bounding wall and dimensionless wall width, are considered and analyzed.

### 2. MATHEMATICAL FORMULATION AND SOLUTION PROCEDURE

The enclosure-modeled room is sketched in Figure 1. The enclosure is bounded by a massive wall with a finite conductivity on the right. A constant heat flux is imposed on the massive wall side to simulate solar radiation input or the convection heat transfer from outdoor airflow. The horizontal boundaries are

<sup>1</sup> Supported by National Natural Science Foundation of China (50578059)

adiabatic and non-diffusive. The left vertical sidewall is of constant heat flux and higher concentration. It is assumed that the dimension in the direction perpendicular of x-y plane is larger enough and the end effects on the flow are negligible, i.e., the flow is two-dimensional, which has verified by Yedder and Bilgen [9].

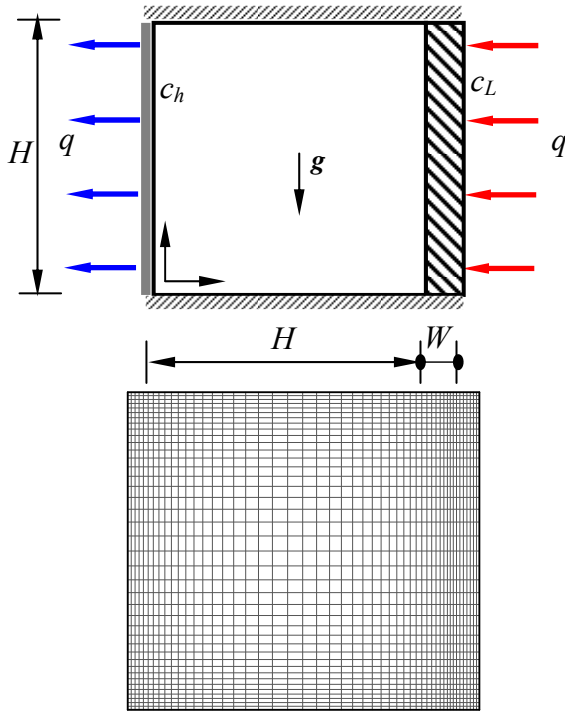


**Fig. 1 Problem geometry, boundary conditions and grid distributions**

The fluid and the pollutant are assumed to be completely mixed, this mixture being the Newton-Fourier fluid fills the cavity, which flows in laminar conditions and does not experience any phase change or chemical reactions. That is to say, the diffusion of contaminants within the building product and the evaporation from the building product surface to the ambient air are maintained on surface of left vertical wall [10]. This fluid is assumed to be incompressible but expands or contracts under the action of temperature and/or concentration gradients. This assumption leads to the Boussinesq approximation if both the temperature and concentration difference levels are maintained within certain limits. The mixture density is assumed to be uniform over the entire cavity, except for the buoyancy term, in which the density is taken as function of both the temperature and concentration

fields. Radiation is negligible. The energy terms of inter diffusive convection and diffusion thermo (Dufour effect) are also not considered [5]. Under these assumptions, the conservative governing equations of continuity, momentum equations are formulated in 2-D Cartesian coordinates described in [4]. The energy and mass transport equations are as follows,

$$\frac{\partial UT}{\partial X} + \frac{\partial VT}{\partial Y} = \frac{\partial}{\partial X}(\lambda_i \frac{\partial T}{\partial X}) + \frac{\partial}{\partial Y}(\lambda_i \frac{\partial T}{\partial Y}) \quad (1)$$

$$\frac{\partial UC}{\partial X} + \frac{\partial VC}{\partial Y} = \frac{\partial}{\partial X}(\gamma_i \frac{1}{Le} \frac{\partial C}{\partial X}) + \frac{\partial}{\partial Y}(\gamma_i \frac{1}{Le} \frac{\partial C}{\partial Y}) \quad (2)$$

Then the conjugate heat and mass transfer could be solved together. In equations (1) and (2), the  $\lambda_i$  and  $\gamma_i$  denote the ratio of thermal conductivities and the ratio of mass diffusivities, the footnote  $i$  represents different zones or materials, 1 and  $Rt$  are set for fluid and thick walls respectively, 1 and  $Rc$  are set for fluid and massive wall respectively. Where,  $Rt$  and  $Rc$  are the heat and mass diffusion coefficient ratios between the material of the separating walls and the medium that fills the cavity. The non-dimensional governing parameters can be formed as,

$$N = \beta_c(c_h - c_L)/\beta_t(t_h - t_L), \quad Ra = \frac{g\beta_t H^3 \Delta T}{\nu_f \alpha_f},$$

$$Pr = \frac{\nu_f}{\alpha_f}, \quad Le = \alpha/D$$

Footnotes  $t, L, h$ , and  $f$  represent referring to heat transfer, low, high and referring to the fluid respectively. These dimensionless variables represent coordinates, velocities, temperature, concentration, buoyancy ratio, pressure, nominal temperature difference, Rayleigh number, Prandtl number and Lewis number. Their detailed physical meanings can be found in [11]. The Prandtl number and thermal Rayleigh number given above are usual when analyzing the single natural convection heat transfer in enclosure. In this way, the buoyancy ratio  $N$  and Lewis number  $Le$  arise, in addition, when analyzing the combined convective heat and mass transfer in

enclosure.  $N$  is the buoyancy ratio, which is the ratio between the solutal and thermal buoyancy forces. It can be either positive or negative, its sign depending on that of the ratio between the volumetric expansion coefficients  $\beta_t$  and  $\beta_c$ . Its limits are that it is null for no pollutant diffusion and infinite for no thermal diffusion. Non-slip conditions are imposed on the walls for velocities, which are zero in solid zone. The horizontal walls are adiabatic and non-diffusive, then the corresponding normal gradient of scalars are set zero. Other boundary conditions are shown Figure 1. The problem under analysis is a conjugate heat and mass transfer problem where it is assumed that, at each interface fluid-horizontal wall of the cavity, the continuities of heat flux and mass flux are satisfied. The above set of differential equations is discretized by Finite Volume Method and solved by the SIMPLE method, using the staggered grids for the velocity components, and integrating the convection-diffusion terms by using the upwind difference scheme. The discretization equations, formally the same for all variables, are solved iteratively with the tri-diagonal matrix algorithm. Over the fluid-solid interface, the conjugated combined heat and mass transfer problem is solved through the use of the harmonic mean practice for the diffusion coefficients [12]. The domain is discretized using the non-uniform rectangular grid, which clusters towards the walls and the interface of fluid and solid. Numerical scheme and boundary conditions are fixed, the mesh is refined by GCI (Grid Convergence Index) to yield a set of numerical parameters [13].

### 3. RESULTS AND DISCUSSIONS

Because the constant heat flux is imposed on the vertical walls, the average Nusselt number of left vertical wall can be defined as,  $Nu = \int I/TdY$ , where  $T$  represents the non-dimensional temperature on the left vertical wall. While the constant mass concentration is imposed on the vertical walls, the average Sherwood number can be defined as,  $Sh = \int -\frac{\partial C}{\partial n} dY$ . The dimensionless parameters governing the conjugated double diffusive transfer problem in square cavity are seven, as shown in the preceding section,  $Pr$ ,  $Ra$ ,  $N$ ,  $W/D$ ,  $Le$ ,  $Rt$  and  $Rc$ . For

the VOC, the  $\beta_c > 0$ , and consequently,  $N > 0$ . The most usual case for building elements,  $Rt \geq Rc$ . In order to obtain a contained work, the results are restricted to these ranges,  $Pr = 0.7$ ,  $Ra = 10^5$ ,  $N = (0-10)$ ,  $W/D = 0.1$ ,  $Le = 0.8$ ,  $Rt (Rc) = 1.0 \times 10^{-4} - 10.0$ .

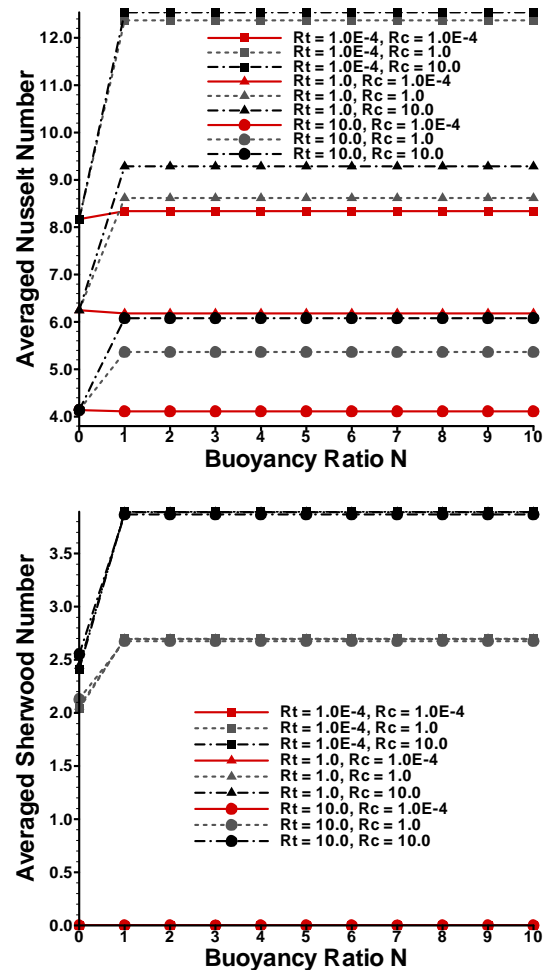


**Fig. 2 Variations of average Nusselt number and Sherwood number with buoyancy ratio**

Figure 2 presents the variations of  $Nu$  and  $Sh$  numbers along with buoyancy ratio  $N$ . Some trends are found. Firstly, the  $Nu$  and  $Sh$  are independent of  $N$  though the average Nusselt and Sherwood numbers increase greatly as  $N$  steps from 0 to 1. As you know, the solutal buoyancy force would be non-existent if  $N$  equals zero. But the solutal transfer would be carried out by the thermal buoyant airflow. Secondly, when  $N$  exceeds 1.0,  $Sh$  is only dependent on the ratio of mass conductivity  $Rc$ , while the  $Nu$  is dependent on the  $Rt$ , also on the  $Rc$ , which are shown in Figure 2,  $Sh$  increases with  $Rc$  and is independent of  $Rt$ , while variations of  $Nu$  show complex. When  $N$  is zero, i.e.,

the thermal convection exists alone, the  $Nu$  is independent of  $Rc$  and decreases with the increased  $Rt$ . As  $N$  is not zero, the  $Nu$  increases greatly with  $Rc$  and decreases with  $Rt$ . As  $Rc$  ranging from 1.0 to 10.0, the difference of  $Nu$  is little, but it increases with  $Rt$ . That is to say, the heat transfer of vertical wall is influenced by thermal-solutal convection, while the mass transfer of vertical wall is mainly influenced by solutal convection. For the two kinds of thermal and mass conditions (constant heat flux and constant concentration), evidently, the latter would impose the major effect on the flow field. Except that, the solutal convection induced from horizontal concentration difference would circle in clockwise direction, the thermal convection induced from temperature difference would oppose the solutal convection and circle in clockwise direction. Therefore, the strengthened solutal convection would damp the thermal convection, even alter or dominate the flow direction. And then heat transfer would decrease with  $Rc$  (noting that the  $Nu$  is reciprocal of temperature). Following that, the flow field and various scalar contours should be presented. When thermal buoyant convection does alone ( $N = 0$ ), the flow fields under different  $Rc$  or  $Rt$  are same for the constant  $Ra$ .

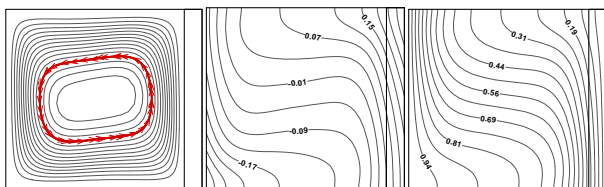
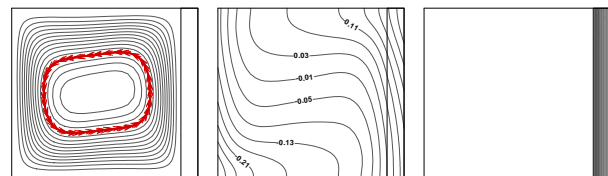


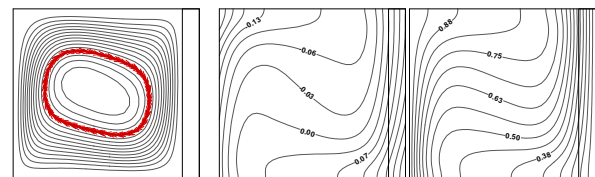
**Fig. 3 Contours of streamline, temperature and concentration ( $N=0$ ,  $Rt=1$  and  $Rc=1$ )**

Then the Figure 3 presents the contours of streamline, temperature and concentration as  $Rt$  and  $Rc$  equal 1.0. Because contours of other cases when  $N$  is zero are similar as those shown in Figure 3, they are not presented. Evidently, the convection driven by thermal buoyant force circles in anti-clockwise. Interestingly, the contour of concentration is similar that of temperature, because the contaminant mass or VOC can be viewed as passive particle transported by the airflow. When  $N$  increases to 1, the corresponding contours are presented in Figure 4. Compared with Figure 3, the streamline has altered direction due to

the dominant solutal buoyant force as  $(Rt, Rc)$  is (1.0, 1.0). As  $Rc$  is low ( $1.0 \times 10^{-4}$ ), the massive wall damps the concentration gradient, then the concentration gradient clusters in the solid zone.



$(Rt, Rc) = (1.0, 1.0 \times 10^{-4})$



$(Rt, Rc) = (1.0, 1.0)$

**Fig. 4 Contours of streamline, temperature and concentration ( $N=1$ ).**

Therefore, the thermal convection dominates once again shown in Figure 4. Seeing from contours of temperature, the temperature gradients are located left and bottom corner on the left vertical wall mainly in Figure 3 and Figure 4 ( $Rc$  is  $1.0 \times 10^{-4}$ ). It notes that the heat transfer happens in the bottom corner near left vertical wall as thermal buoyancy convection is dominant (anti-clockwise streamline). Similarly, as solutal convection is dominant, the concentration gradient clusters in the top corner near left vertical wall. Because the heat or mass conduction goes along the massive wall, then the diagonal corner near the left side of massive wall clustered the temperature or concentration gradient. Therefore, the heat or mass transportation would start or end from/to these zones. If the heatline or massline were adopted, the process would be presented explicitly (Bejan 1995, Costa 1997). As  $(Rt, Rc)$  is (10.0, 10.0), similar contours are encountered, and then they are not shown. When  $N$  increases up to 10, the similar trends as depicted as those in Figure 4, also they are not provided.

Local Nusselt number and Sherwood number on the vertical left wall under some cases are presented in Figure 5. From the local Nusselt distributions, you can discern that the thermal convection is dominant when  $N$  is zero, or when  $N$  is 1 and  $Rc$  equaling  $10^{-4}$ . Therefore the local Nusselt number on top side is larger than that on bottom side. While the other

variations are on the contrary as solutal convection dominates. Except that  $Rc$  is low ( $10^{-4}$ ), the local Sherwood numbers show the mass transfer is mainly encountered on the bottom side as solutal convection dominates ( $N$  equals 1 or 10). But when  $Rc$  is  $10^{-4}$ , the solutal convection does not dominate, then the mass transfer is mainly encountered on the top side shown in Figure 5 (1, 1,  $1.0E-4$ ) noting by ( $N$ ,  $Rt$ ,  $Rs$ ).

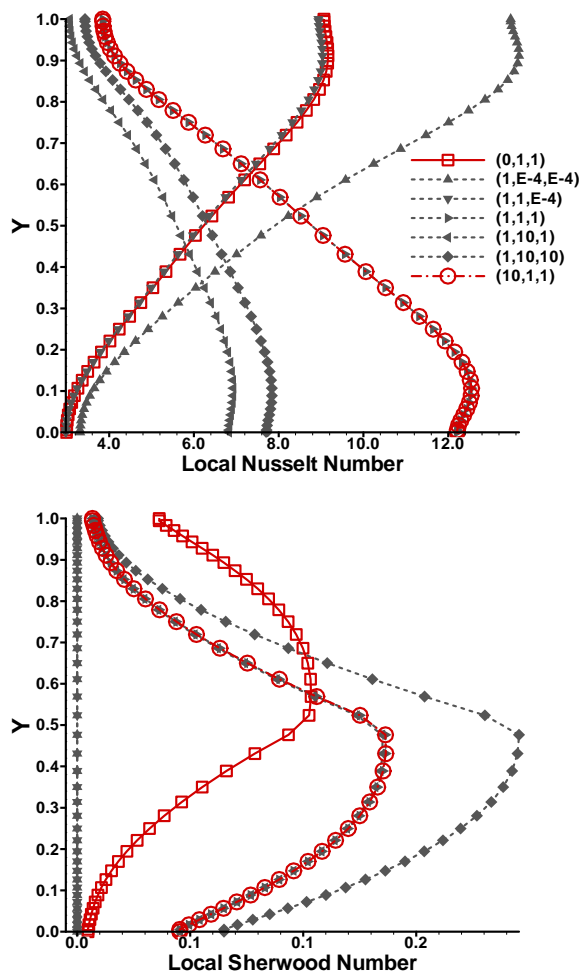


**Fig.5 Local Nusselt number and Sherwood number along with Y on vertical sidewall.**

#### 4. CONCLUSION

Conjugated double diffusive natural convection in square enclosure has been studied. Except the thermal buoyant convection alone, the average Nusselt number and Sherwood number are independent of buoyancy ratio. The average Sherwood number only increases with the ratio of mass conductivity when buoyancy ratio exceeds 1.0, while the average Nusselt number varies with  $Rt$  and  $Rc$ . The direction or dominance of double diffusive

convection lies on the mutual interaction between thermal induced convection and solutal induced convection. First kind boundary condition (constant concentration) would affect the flow more than the second boundary condition (constant heat flux).

#### ACKNOWLEDGMENTS

The authors gratefully acknowledge the financial support of National Natural Science Foundation of China (No. 50578059).

#### REFERENCES

- [1] WOLKOFF P. Volatile organic compounds - sources, measurements emissions and the impact on indoor air quality [J]. *Indoor Air* 1995, (Suppl.3):9-73.
- [2] NAMIESNIK J, GORECKI T, KOZDARON-ZABIEGALA B, LUKASIAK J. Indoor air quality (IAQ), pollutants, their sources and concentration levels [J]. *Building and Environment*, 1992, 27(3):339-356.
- [3] BEGHEIN C, HAGHIGHAT F, ALLARD F. Numerical study of double-diffusive natural convection in a square cavity [J], *International Journal of Heat and Mass Transfer*, 1992, 35:833-846.
- [4] COSTA V A F. Double diffusive natural convection in a square enclosure with heat and mass diffusive walls [J]. *International Journal of Heat and Mass Transfer*, 1997, 40 (17):4061-4071.
- [5] COSTA V A F. Double-diffusive natural convection in parallelogrammic enclosure [J]. *International Journal of Heat and Mass Transfer*, 2004, 47:2913-2926.
- [6] LIAQAT A, BAUTAS A C. Conjugate natural convection in a square enclosure containing volumetric sources [J]. *International Journal of Heat and Mass Transfer*, 2001, 44:3273-3280.
- [7] KIM D M, VISKANTA R. Effect of wall heat conduction on natural convection heat transfer in a square enclosure [J]. *ASME Journal of Heat Transfer*, 1985, 107 (1):139-146.
- [8] DESRAYAUD G, LAURIAT G. A numerical study of natural convection in partially open enclosures with a conducting side wall [J]. *ASME Journal of Heat Transfer* 2004, 126 (1):76-83.
- [9] YEDDER R B, BILGEN E. Turbulent natural convection and conduction in enclosures bounded by

- a massive wall [J]. International Journal of Heat and Mass Transfer 1995, 38 (10):1879-1891.
- [10] KNUDSEN H N, KJAER U D, NIELSEN P A, WOLKOFF P. Sensory and chemical characterization of VOC emissions from building products: impact of concentration and air velocity [J]. Atmospheric Environment 1999, 33 (10):1217-1230.
- [11] BEJAN A. Convection Heat Transfer [M]. New York: Wiley. 1995, 80-82.
- [12] PATANKAR S V. Numerical Heat Transfer and Fluid Flow [M]. New York: McGraw-Hill. 1980, 126-128.
- [13] ROACHE P J. Perspective: a method for uniform reporting of grid refinement studies [J]. ASME Journal of Fluids Engineering 1994, 116:405- 413